

Crack-free and conductive Si-doped AlN/GaN distributed Bragg reflectors grown on 6H-SiC(0001)

Tommy Iwe,^{a)} Oliver Brandt, Helmar Kostial, Thorsten Hesjedal, Manfred Ramsteiner, and Klaus H. Ploog
Paul-Drude-Institut für Festkörperelektronik, Hausvogteiplatz 5-7, D-10117 Berlin, Germany

(Received 1 June 2004; accepted 11 July 2004)

We demonstrate Si-doped *n*-type AlN/GaN distributed Bragg reflectors grown on 6H-SiC(0001). The structures are crack-free and have a stopband centered around 450 nm with a full width at half maximum between 40 and 50 nm. The maximum measured reflectance is $\geq 99\%$. A comparison between Si-doped and undoped structures reveals no degradation of the reflectance due to the Si doping. Vertical conductance measurements at room temperature on the samples show an ohmic *I*-*V* behavior in the entire measurement range. The measured resistivity at 77 K is only a factor of 2 larger than the resistivity measured at room temperature. © 2004 American Institute of Physics. [DOI: 10.1063/1.1791738]

For devices such as resonant-cavity light-emitting diodes and vertical-cavity surface emitting lasers (VCSELs), which rely on distributed Bragg reflectors (DBRs), it would be highly desirable if the DBRs themselves were vertically conductive. Otherwise, one has to use lateral current injection that requires additional *ex situ* processing steps for defining a current aperture. These additional steps would be made redundant with DBRs that allow vertical current injection. AlN and GaN are the preferred materials for the realization of nitride-based DBRs for the blue and green spectral range because of their comparatively large refractive index contrast ($\Delta n/n=0.16$). However, so far there have been no reports concerning doped GaN/AlN-DBRs, presumably because AlN is commonly believed to be invariably insulating by nature. In addition, the huge conduction band offset between GaN and AlN (2.2 eV) seems to completely hinder a carrier flow across the heterointerfaces. Furthermore, the large lattice mismatch between GaN and AlN (2.4%) often leads to crack formation, due to the accumulation of tensile strain in these structures.¹ Cracks have a detrimental effect on the reflectivity and they make electronic-device processing basically impossible. In order to circumvent crack formation, a variety of successful approaches to reduce the strain in nitride-based DBRs have been reported, such as growth of strain-balanced buffer layers,²⁻⁴ AlN-insertion layers,⁵ reducing the lattice mismatch⁶⁻⁹ by growing $\text{Al}_x\text{Ga}_{1-x}\text{N}/\text{Al}_y\text{Ga}_{1-y}\text{N}$ and growth of lattice-matched (Al,In)N/GaN DBRs.¹⁰

In this work, we report on the growth of both undoped and homogeneously Si-doped ($[\text{Si}]=1-2 \times 10^{19} \text{ cm}^{-3}$) AlN/GaN-DBRs on 6H-SiC(0001) by plasma-assisted molecular beam epitaxy (PAMBE). Each DBR consists of 20.5 periods of nominally 47 nm GaN and 57 nm AlN designed for a peak reflectance of $\geq 99\%$ at 450 nm according to the $\lambda/4$ criterion. Our structures are found to be crack-free by interference-contrast optical microscopy, scanning electron microscopy (SEM), and atomic force microscopy (AFM). In addition, vertical conductivity measurements show that our Si-doped DBRs are conducting.

The employed PAMBE system was assembled by VTS-CreaTecTM, and is equipped with solid-source effusion cells for Al, Ga, and Si and an SVTTM radio-frequency nitrogen plasma source for producing active N. The system has a base pressure of 5×10^{-11} Torr. We use 6N N₂ gas as a precursor, which is further purified to 5 ppb by a getter filter. Conducting *n*-type ($10^{-3} \Omega \text{ cm}$) 6H-SiC(0001) wafers were used as substrates. The substrate temperatures given in the following were calibrated by visual observation of the melting point of Al (660 °C) attached to the substrate as well as by pyrometry. In order to remove residual suboxides from the SiC substrate surface, an *in situ* Ga flash-off procedure was performed prior to growth.¹¹ The structures were grown directly on the 6H-SiC substrate without employing a buffer layer. Metal-stable growth conditions at 780 °C were used, yielding N-limited growth rates of 450 nm/h for both AlN and GaN. Since the growth rate is determined by the (constant) N flux, the individual layer thickness can be directly derived from the period. We used a Philips X'Pert ProTM triple-axis x-ray diffractometer with a Si(022) analyzer crystal to determine the period with an accuracy of ± 0.5 nm. During growth a streaky reflection high-energy electron diffraction (RHEED) pattern was observed, indicating a smooth surface. Each GaN layer was followed by a 10 s growth interruption which was increased to 30 s after an AlN layer. These growth interruptions allowed for excess metal to desorb, observed as an abrupt low-to-high intensity transition of the RHEED pattern prior to starting the growth of a new layer. The Si concentration was adjusted between $1-2 \times 10^{19} \text{ cm}^{-3}$ by varying the Si effusion cell temperature.

A Filmetrics F20TM reflectometer was used to measure the reflectivity of the DBRs. We investigated the surface morphology using a Park-ScientificTM AFM operating in contact mode. Raman spectroscopy was done in the back-scattering configuration using a He-Ne laser emitting at 632.8 nm. For the electrical measurements, mesa structures of different diameters (70, 230, and 450 μm) were prepared using photolithography and Ar/Cl₂ reactive-ion etching. Rear (substrate) and front (DBR) contacts were made by electron-beam evaporation of Ni/Cr followed by deposition of Au for a total contact thickness of 165 nm. The contacts were alloyed at 750 °C for 5 min. The etching was done in

^{a)} Author to whom correspondence should be addressed; electronic mail: iwe@pdi-berlin.de

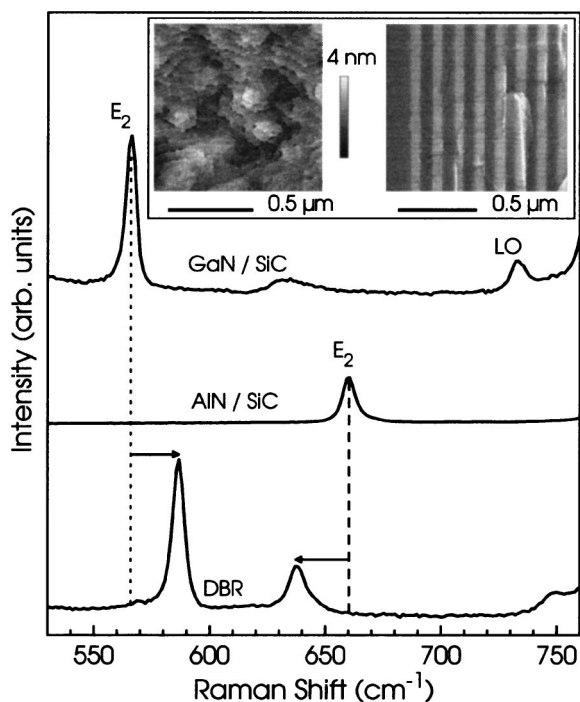


FIG. 1. Raman spectra of thick GaN (top) and AlN (center) films and an undoped DBR structure (bottom). The left picture in the inset shows an AFM micrograph of the surface of an undoped DBR taken over a $1 \times 1 \mu\text{m}^2$ area. The right picture in the inset shows an SEM image of a cross section (sideview) of the undoped DBR in Fig. 1.

sequences in order to allow for measuring the conductivity at different depths. Dynamic contact electrostatic force microscopy¹² (DC-EFM) was used to electrically probe the sample surfaces. This technique does not require a conducting path between tip and sample and allows simultaneous AFM characterization of the surface morphology.

To elucidate the reason for the absence of cracks in our structures, we performed Raman spectroscopy, which provides information about the strain state of the constituent GaN and AlN layers. Figure 1 shows a comparison of Raman spectra of thick GaN (top) and AlN (center) films with that of a DBR (bottom). The measured positions of the E_2 phonon peaks of the thick GaN (566.3 cm^{-1}) and AlN (662.2 cm^{-1}) films are in good agreement with values found in the literature and consistent with a slight compressive and tensile strain, respectively.^{13–15} However, in the case of the DBR, the position of the E_2 phonon peak of GaN (dotted line) shifts to higher wave numbers ($+20.5 \text{ cm}^{-1}$), reflecting a strong compressive strain ($-1.3\% \pm 0.2\%$).^{13,15} The position of the E_2 phonon peak of AlN (dashed line), on the other hand, shifts towards lower wave numbers (-23.0 cm^{-1}), which signifies an equally strong tensile strain ($+1.3\% \pm 0.2\%$).^{14,15} Since the GaN and AlN layers experience opposite strain of virtually equal magnitude, the structure approaches a strain-compensated state with the residual net stress being close to zero. This drastically lowers the likelihood of crack formation. The cause of this strain compensation is that the first GaN and AlN layers are thin enough to only partially relax. The left picture in the inset of Fig. 1 shows an AFM micrograph of the surface of an undoped DBR taken over a $1 \times 1 \mu\text{m}^2$ area. A very smooth surface morphology with clearly resolved monolayer steps can be observed. The right picture in the same inset shows an

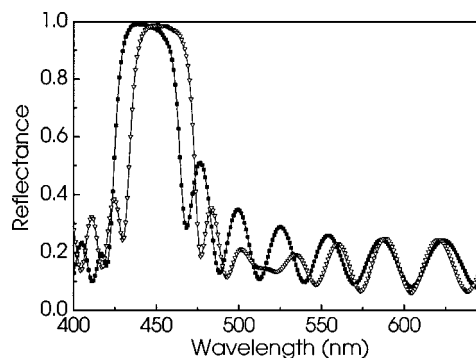


FIG. 2. Reflectance spectra of an undoped DBR (filled squares) and a doped DBR (open triangles).

SEM image of a cross section (sideview) of the first 7.5 periods of another undoped sample. The leftmost (bottom) layer constitutes the SiC/GaN boundary. We see that the alternating GaN (bright) and AlN (dark) layers exhibit abrupt and smooth interfaces. Larger-scale images (not shown here) show that the interfaces remain abrupt and smooth throughout the more than $2\text{-}\mu\text{m}$ -thick structure.

Figure 2 shows the reflectivity spectra of both an undoped (filled squares) and a doped (open triangles) DBR. Both samples have a reflectivity $\geq 99\%$ with a stopband centered around 450 nm (454 and 445 nm, respectively). The full width at half maximum (FWHM) of the stopband is 40 nm for the undoped and 41 nm for the doped DBR. It is important to note that the Si-doping does not degrade the reflectivity. The AlN and GaN layer thicknesses of the undoped sample (46.4 and 56.9 nm, respectively) are slightly larger than those of the doped sample (45.3 and 55.8 nm, respectively). This causes the small shift of the stopband observed in Fig. 2. The results of our reflectivity measurements have been confirmed by variable-angle spectroscopic ellipsometry,¹⁶ which provides an absolute reflectivity and shows that our reflectometer is well calibrated.

Figure 3 shows the vertical I - V characteristics of a DBR with a Si-doping concentration of $1.1 \times 10^{19} \text{ cm}^{-3}$. The measurement was done at room temperature using two different contact diameters, each corresponding to one of the curves in Fig. 3, showing that the structure is ohmic in the entire measurement range. The specific series resistance R_0A of this sample is $4 \times 10^{-3} \Omega \text{ cm}^2$ compared to $2 \times 10^{-3} \Omega \text{ cm}^2$ for

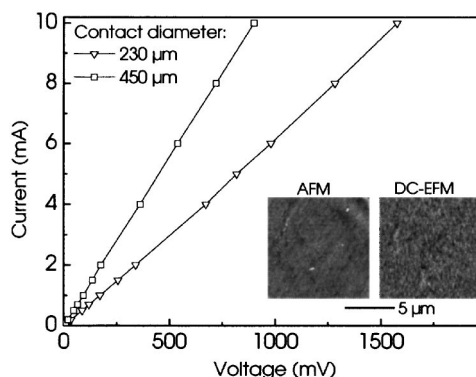


FIG. 3. Vertical I - V measurements of a doped DBR done at room temperature using two different contact diameters. The right image in the inset shows a DC-EFM map of the surface of a doped DBR taken over a $10 \times 10 \mu\text{m}^2$ area. The left image shows the corresponding AFM micrograph of the same area.

another sample Si-doped to a level of $1.6 \times 10^{19} \text{ cm}^{-3}$. In contrast, the undoped DBRs exhibit a resistance which is at least four orders of magnitude higher than that of the doped DBRs. Etching experiments on the conducting DBRs show that the vertical resistance varies linearly with depth. Furthermore, the resistance of the doped structures measured at 77 K is only a factor of 2 larger than that measured at 300 K, indicating that no significant carrier freeze-out occurs. Thus, these structures exhibit a metalliclike behavior.

This metalliclike conductivity gives rise to concern about the possible presence of highly conducting channels in the doped DBRs, perhaps provided by open-core screw dislocations decorated by Ga or Al (the absence of such channels in undoped DBRs would, however, be difficult to understand). The right image of the inset of Fig. 3 shows the results of a representative DC-EFM measurement made over a $10 \times 10 \mu\text{m}^2$ area of a DBR with a doping concentration of $1.6 \times 10^{19} \text{ cm}^{-3}$. No conducting channels were observed within the lateral resolution of the measurement (approximately 70 nm). Thus, the picture only reflects the measurement noise. The few small areas of higher contrast (black) can be ascribed to surface contamination since they correlate with the positions of the bright spots seen in the left image of the inset, corresponding to the AFM micrograph recorded simultaneously. Our x-ray results show that the density of screw dislocations¹⁷ ($\leq 10^9 \text{ cm}^{-2}$) translates to an average distance of at least 0.3 μm between two screw dislocations. Since only pure screw dislocations are associated with leakage current paths in GaN,^{18,19} the presence of such current paths would have been revealed in the DC-FEM scans. To clarify the origin of the high conductivity of the Si-doped DBRs, we investigated the electrical properties of thick AlN:Si layers grown on 6H-SiC(0001) by PAMBE. Temperature-dependent Hall measurements show that the AlN:Si layers are indeed semiconducting in contrast to undoped AlN samples, which are insulating.²⁰ Self-consistent Schrödinger-Poisson simulations of the band profile reveal that the GaN layers are degenerate, and that all donors in AlN are autoionized due to charge transfer. However, when taking into account the full theoretical polarization charges at the heterointerfaces, the triangular AlN depletion region is too wide to allow for any appreciable tunneling across the interfaces. Nevertheless, interface states could partly compensate this polarization charge, which would drastically re-

duce both the height and the width of the AlN tunneling barrier, thereby making tunneling possible.

To conclude, we show that it is possible to achieve crack-free and vertically conducting GaN/AlN DBRs with a very high reflectivity. These structures are promising for use as an *in situ* grown integral component of nitride-based VCSELs.

The authors would like to thank Hans-Peter Schönherr, Michael Hörické, and Claudia Hermann for invaluable technical assistance.

¹H. M. Ng, T. D. Moustakas, and S. N. G. Chu, *Appl. Phys. Lett.* **76**, 2818 (2000).

²A. Thamm, O. Brandt, K. H. Ploog, J. Hilsenbeck, and R. Lossy, in *27th International Symposium on Compound Semiconductors*, edited by M. Melloch and M. A. Reed (IEEE, Piscataway, NJ, 2000), p. 455.

³F. Natali, D. Byrne, A. Dussaigne, N. Grandjean, J. Massies, and B. Damilano, *Appl. Phys. Lett.* **82**, 499 (2003).

⁴A. Bhattacharyya, S. Iyer, E. Iliopoulos, A. V. Sampath, J. Cabalu, T. D. Moustakas, and I. Friel, *J. Vac. Sci. Technol. B* **20**, 1229 (2002).

⁵K. E. Waldrip, J. Han, J. J. Figiel, H. Zhou, E. Makarona, and A. V. Nurmikko, *Appl. Phys. Lett.* **78**, 3205 (2001).

⁶S. Fernández, F. B. Naranjo, F. Calle, M. A. Sánchez-García, E. Calleja, P. Vennegues, A. Trampert, and K. H. Ploog, *Appl. Phys. Lett.* **79**, 2136 (2001).

⁷N. Nakada, M. Nakaji, H. Ishikawa, T. Egawa, M. Umeno, and T. Jimbo, *Appl. Phys. Lett.* **76**, 1804 (2000).

⁸T. Someya and Y. Arakawa, *Appl. Phys. Lett.* **73**, 3653 (1998).

⁹O. Ambacher, M. Arzberger, D. Brunner, H. Angerer, F. Freudenberg, N. Esser, T. Wethkamp, K. Wilmers, W. Richter, and M. Stutzmann, *MRS Internet J. Nitride Semicond. Res.* **2**, 22 (1997).

¹⁰J.-F. Carlin and M. Ilegems, *Appl. Phys. Lett.* **83**, 668 (2003).

¹¹O. Brandt, R. Muralidharan, P. Waltereit, A. Thamm, A. Trampert, H. von Kiedrowski, and K. H. Ploog, *Appl. Phys. Lett.* **75**, 4019 (1999).

¹²E. Z. Luo, J. B. Xu, W. Wu, I. H. Wilson, B. Zhao, and X. Yan, *Appl. Phys. A: Mater. Sci. Process.* **66**, S1171 (1998).

¹³P. Waltereit, O. Brandt, A. Trampert, M. Ramsteiner, M. Reiche, M. Qi, and K. H. Ploog, *Appl. Phys. Lett.* **74**, 3660 (1999).

¹⁴J. Gleize, M. A. Renucci, J. Frandon, E. Bellet-Amalric, and B. Daudin, *J. Appl. Phys.* **93**, 2065 (2003).

¹⁵A. R. Goñi, H. Siegle, K. Syassen, C. Thomsen, and J.-M. Wagner, *Phys. Rev. B* **64**, 035205 (2001).

¹⁶R. Goldhahn, T. Ive, O. Brandt, *et al.* (unpublished).

¹⁷Y. J. Sun, O. Brandt, T. Y. Liu, A. Trampert, K. H. Ploog, J. Bläsing, and A. Krost, *Appl. Phys. Lett.* **81**, 4928 (2002).

¹⁸B. S. Simpkins, E. T. Yu, P. Waltereit, and J. S. Speck, *J. Appl. Phys.* **94**, 1448 (2003).

¹⁹J. Spradlin, S. Doğan, J. Xie, R. Molnar, A. A. Baski, and H. Morkoç, *Appl. Phys. Lett.* **84**, 4150 (2004).

²⁰T. Ive, O. Brandt, and K. H. Ploog (unpublished).